Detailed Materials and Methods

Behavioral experiments. Mice were subjected to a series of behavioral tests as described before (Kerimoglu, Agis-Balboa et al. 2013). In all instances animals were tracked with the TSE monitoring system Videomot2. Briefly, for the open field, mice were introduced in an empty, square, plastic box for 5min and allowed to freely explore the arena. Time spent in the center was recorded. For elevated plus maze, mice were introduced in a 4-arm maze with two open and two closed arms. Mice were tracked with TSE's Videomot2 system and time spent in the open arms was recorded. For Morris Water Maze (MWM), mice were trained for the indicated time to find a hidden platform in a circular pool filled with opaque water. Mice were given 4 training trials per day in which they were allowed to navigate the pool for 1min. Animals that did not find the platform were gently guided to it and allowed to stay on the platform for 15sec prior to the next trial. The insertion point for each trial was randomized daily. On testing days (probe trials), the platform was removed and mice were introduced in the pool at the position opposite to the original location of the platform. They were allowed to explore the pool for 1min. Every day, mice were tracked and the latency to reach the platform or the percentage of time spent in the target quadrant were recorded.

Mouse cannulation and injections. 10-week old C57B/6JRj mice were ordered from Janvier and allowed one week to habituate to the animal facility prior to any handling. Two days prior to and following the operation, mice were given oral Metamizol (3ml/liter) to minimize pain and stress during the procedure. On the day of cannulation, mice were anesthetized with a ketamine (80 mg/kg)/xylazine (10 mg/kg) mixture, fixed on a stereotaxic device (myNeuroLab) and openings were drilled at the following coordinates: antero-posterior: -1.75; medio-lateral: +/- 1. Cannulae (1.5mm long) were then implanted and fixed with dental cement. Mice were given a week recovery time prior to starting behavioral experiments. Mice were then trained in the Morris Water Maze as described above and received daily bilateral injections of spliceostatin (AdooQ) after each training session (consisting of four trials). Mice were anesthetized with isofluorane and 1µl spliceostatin was injected at a concentration of 190nM in 0.9% NaCl at a rate of 0.5µl/min.

Tissue dissection and RNA isolation. Mice were sacrificed by cervical dislocation and the brain was quickly isolated on ice. CA1/DG dissection was performed according to (Hagihara, Toyama et al. 2009). Tissue was snap-frozen in liquid nitrogen and stored at -80C until processing. For RNA extraction, tissue was homogenized in Tri reagent (Sigma) and RNA was extracted according to manufacturer's instructions. RNA was treated with DNaseI prior to sequencing. Briefly, RNA was resuspended in water and treated with 2U of DNaseI (Invitrogen) for 20min at 37C. DNA-free RNA was then repurified with Phenol:Chloroform and resuspended in DEPC water according to standard protocols. RNA was stored at -80C.

Western blotting. For STAT1 analysis, protein was extracted from the Tri reagent organic phase after RNA isolation as follows: DNA was precipitated with ethanol and the remainder mix of tri-ethanol dialyzed against 0.1% SDS in water overnight at 4C in 1kDa MWCO pre-wetted dialysis tubing (Spectrumlabs, Ref. 132636). The proteinic mass was then resuspended in TX buffer (50mM Tris-HCl, 150nM NaCl, 2mM EDTA, 1% Triton-X, pH 7.4) containing 1% SDS and loaded onto a 12% SDS-PAGE gel, separated and transferred onto nitrocellulose membrane with a semi-dry system (BioRad). Membranes were blocked with 5% BSA in TBST (TBS + 0.1% Tween-20) for 1h at room temperature and incubated in the indicated antibodies at different dilutions (pSTAT1 (Cell Signaling), 1:250; Actin (Santa Cruz): 1:1000) in 5% BSA in TBST overnight at 4C. They were washed 3x with TBST for 10min at RT and incubated with IRDye secondary antibodies (LI-COR) at 1:5000 in 5% BSA for 1h in the dark at RT. Membranes were then washed 3x with TBST and scanned and quantified in an Odyssey CLx LI-COR scanner. For CLK1 analysis, 3- and 16-month old animals were sacrificed and the CA1 region was dissected. Nuclear protein was extracted following the manufacturer's instructions from the ProteoExtract (Calbiochem) kit. The blotting procedure was as above with the CLK1 antibody (Novus) used at a concentration of 1:50.

FACS sorting. Tissue from 4-7 animals was pooled for every replicate for two replicates per condition with the exception of the following conditions, where a single replicate (nonetheless comprised of 4-7 animals) was possible due to tissue limitations: WT veh glia H4K12 ChIP; WT veh neuron input; WT veh glia input. Tissue was homogenized in low sucrose buffer (0.32M sucrose, 5mM CaCl2, 5mM Mg(Ac)2, 0.1mM EDTA, 50mM HEPES pH8, 1mM DTT, 0.1% Triton X-100) and fixed with 1% PFA for 10min at RT in a rotating wheel. PFA was quenched with 125mM glycine for 5min at RT in a rotating wheel. The suspension was centrifuged at 1000 x g for 3min at 4C, nuclei were resuspended in low sucrose buffer and homogenized with a mechanical homogenizer (IKA Ultra Turrax). The homogenized solution was layered on top of a high sucrose buffer (1M sucrose, 3mM Mg(Ac)2, 10mM HEPES, pH 8.0, 1mM DTT) and centrifuged at 4000 x g 10min at 4C to recover the pelleted nuclei. Nuclei were resuspended in PBTB (PBS, 5%BSA, 0.1% Tween-20) and stained with NeuN antibody (Millipore, Ref. MAB377) in the presence of goat serum in a rotating wheel for 30min at 4C. Samples were washed twice PBTB and stained with a secondary antibody (Life Technologies, Alexa Fluor® 488) for 15min at 4C in a rotating wheel. They were then washed once with PBST (PBS, 0.1% Tween-20) and sorted in a FACS Aria II instrument (BD Biosciences) according to standard procedures.

ChIP assay. All procedures were carried out in DNA low binding tubes from Eppendorf or Diagenode where indicated. Sorted nuclei were lysed in RIPA-SDS (140mM NaCl, 1mM EDTA, 1% Triton-X-100, 0.1% sodium deoxycholate, 10mM Tris-HCl, pH8, 1%SDS) buffer for 10min at 4C in a rotating wheel in sonication tubes (Diagenode). They were then sonicated

20min in a Bioruptor plus NGS (Diagenode) at high setting. Samples were spun down every 4 cycles to ensure homogeneous sonication of the sample. Chromatin was centrifuged at 18000 x g 5min at 4C and the supernatant was snap frozen as sheared chromatin. A small sample was checked for efficient sonication in a Bioanalyzer (Agilent) and used to estimate chromatin concentration in the sample after reversion of crosslinking, which was achieved by treating samples with 0.1µg/µl RNaseA (Qiagen) and then digesting protein with proteinase K (PK, Roth). Chromatin was precleared by diluting it to 10x the initial volume in IP buffer (150mM NaCl, 1% NP40, 0.5% sodium deoxycholate, 50mM Tris-HCl pH8, 20mM EDTA, 0.1% SDS), adding 20µl of magnetic Dynabeads (Life Technologies) and incubating the mix at 4C for at least 4h in a rotating wheel. For H4K12ac ChIPs, 500µg of precleared chromatin and 0.5µg of anti-H4K12ac antibody (abcam Ref. ab61238) were allowed to interact overnight at 4C in a rotating wheel. IP'ed chromatin was then recovered by adding 15µl of magnetic Dynabeds and incubating further 2h at 4C in a rotating wheel. Samples were then washed with 2x with IP buffer, 3x with wash buffer (100mM Tris-HCl pH8, 500mM LiCl, 1% NP40, 1% sodium deoxycholate, 20mM EDTA), 2x with IP buffer and 2x with TE buffer (10mM Tris-HCl, 1mM EDTA). Samples were kept on ice at all times. Beads were collected with a magnetic stand (Invitrogen). After the last wash, IP and input samples (input samples constituted 10% of the material used for ChIP) were collected and eluted in 20µl EB buffer (10mM Tris-HCl pH8) containing 0.1µg/µl RNaseA and incubated at 37C for 30min under gentle agitation in a Thermomix (Eppendorf). Samples were then further diluted ½ with WB buffer (100mM Tris-HCl pH8, 20mM EDTA, 2% SDS) and 1µl of PK (20mg/ml) was added. Samples were then incubated overnight at 65C under agitation in a Thermomix. DNA was recovered on the magnetic stand and re-eluted with EB buffer for 10min at 65C. Inputs were carried in parallel after the IP. DNA was precipitated with SureClean (Bioline) and linear polyacrylamide (LPA, Bioline), washed 2x with 70% EtOH and quantified using the Qubit (Life Technologies).
All buffers were supplemented with a proteinase inhibitor cocktail (Roche, Ref. 04 693 132 001)

RNASeq, small RNASeq, ChIPSeq and bioinformatical analysis. Library preparation and cluster generation for mRNA sequencing was performed according to Illumina standard protocols (TruSeq, Illumina). Libraries were quality-controlled and quantified using a Nanodrop 2000 (Thermo Scientific), Agilent 2100 Bioanalyzer (Agilent Technologies) and Qubit (Life Technologies). Small RNA library preparation and sequencing was performed analogously.
Base calling from raw images and file conversion to fastq files was achieved by Illumina pipeline scripts. Subsequent steps included quality control (FastQC, www.bioinformatics.babraham.ac.uk/projects/fastqc/), mapping to reference genome (mm10, STAR aligner v2.3.0, (Djebali, Davis et al. 2012) non-default parameters), read counting on genes or exons (HTSeq, http://www-huber.embl.de/users/anders/HTSeq, mode: intersection-non-empty) and differential gene (DESeq2_1.4.5 (M. I. Love 2014)) or exon (DEXSeq_1.10.8

(Anders, Reyes et al. 2012)) usage biostatistical analysis. PCA and distance heatmaps were generated in R following instructions in the vignette for DESeq2. Genes were considered differentially expressed with an adjusted (Benjamini-Hochberg) p-value<0.05. Gene set overlaps were calculated using Venny (http://bioinfogp.cnb.csic.es/tools/venny/). Gene Ontology (GO) functional analysis was carried out using Webgestalt unless otherwise stated (http://bioinfo.vanderbilt.edu/webgestalt/, (Zhang, Kirov et al. 2005)). The Database for Annotation, Visualization and Integrated Discovery (DAVID, v6.7) (Huang, Sherman et al. 2009) was used for functional exploration of differential exon usage in old animals. For Webgestalt analyses of aged animals, only genes with a p<0.01 were used as input. For Webgestalt analysis of APP/PS1-21 animals, a p-value cutoff of 0.00001 and log2FC cutoff of 1 (for upregulated) and -0.2 (for downregulated) genes was used to limit the number of genes to input for analysis to limit the input to the most significant genes. For DAVID analysis, only genes with exons that had a log2FC>|0.2| and pval<0.05 were used as input. GO categories were collapsed into "slim terms" (option "MGI Slim 2" that excludes general categories) using CateGOrizer (Hu Zhi-Liang 2008). For stringency purposes, only the first (according to significance) 200 GO categories were input to CateGOrizer. TFBS analysis was carried out using PSCAN (http://159.149.160.51/pscan/ (Zambelli, Pesole et al. 2009)). Only genes with a 1.5 fold change cutoff were used for the analysis, and the region from -200 to +50 and JASPAR databases were used as parameters. For ChIP-Seq analysis, replicates were merged into a single file using SAMtools' (Li, Handsaker et al. 2009) function *merge*. Duplicate reads were removed using SAMtools' *rmdup*. Coverage per position was calculated using R packages GenomicRanges (GenomicRanges_1.16.3, (Lawrence, Huber et al. 2013)) and GenomicFeatures (GenomicFeatures_1.16.1, (Kuroda, Kutner et al. 2009)) and plotted in R. Read counts for IP and input samples were normalized to their total count and the IP signal was normalized to the respective input.

Aβ stainings and quantification. Mice were anesthetized with a lethal dose of ketamine/xylazin (100mg/kg; 150mg/kg) and perfused with cold PBS. Brains were fixed in 4% PFA for 3 days at 4C and transferred to a 20% sucrose solution prior to freezing and storage at -80C. They were then sliced at 40 µM with a Cryostat (Leica) and stained with Thioflavin S with the following procotol: slices were rinsed once with PBS, incubated with 0.05% Thioflavin S in 50% EtOH for 8min in the dark and differentiated with 2x washes in 80% EtOH for 10sec each. They were then washed 2x with distilled water and incubated in a high phosphate concentration buffer (411mM NaCl, 8.1mM KCl, 30mM Na2HPO4, 5.2 mM KH2PO4, pH7.2) at 4C for 30min and rinsed with PBST (PBS, 0.1% Tween-20). Finally, they were counterstained with DAPI and mounted on glass coverslips. Images were obtained with an Olympus IX70 microscope. At least 3 slices per mouse and 4-5 mice per group were used for quantification. Quantification was done in ImageJ. Background subtraction was performed and a threshold binning was set from 26 to 255. Images were inspected and an arbitrary minimum particle size 100 was set to include small particles and exclude potential artifacts

from the staining. Particles were then counted and quantified with ImageJ's "analyze particles" function.

Slice Preparation and Electrophysiology Hippocampal slices were prepared as described previously (Ramachandran and Frey 2009) from 8-10 week-old male C57BL/6 mice purchased from Janvier. Animals were anesthetized with isoflurane and decapitated. The hippocampus was removed from the brain and 400 µm thick slices were cut transversely from the dorsal hippocampus in ice-cold artificial cerebrospinal fluid (ACSF) containing (in mM) 124 NaCl, 4.9 KCl, 1.2 KH_2PO_4, 2.0 $MgSO_4$, 2.0 $CaCl_2$, 25.6 $NaHCO_3$,10.0 D-glucose (saturated with 95% O_2 and 5% CO_2, pH 7.4, ~305 mOsm), using a tissue chopper (Stoelting). Slices were incubated in an interface chamber (volume 2 ml) at 32^o C and high oxygen tension was maintained by bubbling with 95% O_2 and 5% CO_2 (30 l/h). Slices were perfused with ACSF at 0.76 ml/min, and allowed to recover for 3h after preparation. Then, monopolar lacquer-coated stainless steel electrodes (571000, A-M Systems), used for both recording and stimulating, were positioned in the CA1 region. The field excitatory postsynaptic potential (fEPSP) slope was recorded with a Model 1700 differential AC amplifier (A-M Systems) and Power 1401 analog-to-digital converter (Cambridge Electronic Design), and monitored online with the custom-made software, PWIN (IFN Magdeburg). The test stimulation strength was determined for each input as the current needed to elicit a field EPSP of 40% maximal slope. Baseline recording began at least 3.30 h after slice preparation, using test stimuli consisting of four biphasic constant current pulses (0.2 Hz, 0.1 ms/polarity, averaged) per time point, every 5 min for a minimum of 30 min. LTP was induced with a strong tetanization protocol consisting of three stimulus trains (100 biphasic constant-current pulses per train at 100 Hz and 0.2 ms/polarity, inter-train interval 10 min). Test stimuli were delivered 1, 3, 5, 11, 15, 21, 25, and 30 min after the first tetanization train and then every 5 min for up to 2 h. Drugs (spliceostatin 190nM, SAHA 10µM) were delivered starting 1h prior to LTP induction and throughout the experiment.

Supplementary Figure Legends

Figure S1. SAHA does not cause motor or anxiety side effects. A. Explorative behavior as measured in the open field is not significantly altered amongst groups (t-test, n = 17 (YV), 22 (OV), 20 (OS)). **B.** The percentage of time spent in the open arms of the elevated plus maze is not significantly altered amongst groups. n = 16 (YV), 19 (OS), 18 (OS). Error bars indicate S.E.M.

Figure S2. SAHA normalizes hippocampal gene expression in aged animals. A. Heatmap showing genes significantly altered between the OV and YV groups. Columns represent genes and row individual samples. **B.** Principal component analysis of young and aged vehicle- and SAHA-treated animals shows a clear separation between young and old mice. SAHA-treated old animals cluster closer to young vehicle-treated mice than to aged vehicle-treated animals. **C-D.** Main functional categories associated with genes that are upregulated (**C**) or downregulated (**D**) in aged mice treated with vehicle (OV) or SAHA (OS).

Figure S3. CLK1 protein levels are decreased in 18-month old animals. CLK1 levels were analyzed in nuclear lysates from the hippocampal CA1 region of via quantitative immunoblot analysis using the Odyssey CLx LI-COR scanner (3 vs 18-month of age). * $p < 0.05$ t-test, n = 5 (3-month old) and n = 9 (18-month old). Error bars indicate S.E.M.

Figure S4. Ageing and SAHA affect differential exon usage. The expression of exons identified to be differentially regulated in the CA1 region from aged mice was confirmed via qPCR analysis in all three experimental groups. Namely, YV; young vehicle treated; OV, old vehicle treated and OS, old SAHA treated mice. The upper panel shows qPCR results for exons that were identified to be significantly different via RNA-sequencing and the lower panel shows qPCR results from exons within the same gene that did not significantly differ in the RNA-sequencing analysis. Numbers inside the bars indicate the n number for each group. * $p < 0.05$ t-test.

Figure S5. The *Nptn* locus as an example of age-associated differential promoter usage. The left panel showns the *Nptn* locus comparing exon usage in 3 (young_veh) and 18-month old mice treated with vehicle (old_veh). The right panel shows the *Nptn* locus comparing exon usage in 3 (young_veh) and 18-month old mice treated with SAHA (old_SAHA). Note that the significant increase in exon usage seen in aged mice is normalized after SAHA treatment. * $p < 0.05$ Generalized Linear Model (GLM), n = 8 (YV), 6 (OV), 6 (OS).

Figure S6. The *Sptbn1* locus as an example of age-associated alternative splicing. The The left panel shows the *Sptbn1* locus comparing exon usage in 3 (young_veh) and 18-month old mice treated with vehicle (old_veh). The right panel shows the *Sptbn1* locus comparing exon usage in 3 (young_veh) and 18-month old mice treated with SAHA (old_SAHA). Note that the significant increase in exon usage seen in aged mice is normalized after SAHA treatment. * $p < 0.05$ GLM, n = 8 (YV), 6 (OV), 6 (OS). Arrow indicates the significant exon that is suggestive of a higher usage of the shorter isoforms of the gene. Importantly, some of these isoforms have distinct N- and C-termini and lack important functional domains.

Figure S7. The *Usp21* locus as an example for age-associated nonsense-mediated decay. The left panel shows the *Usp21* locus comparing exon usage in 3 (young_veh) and 18-month old mice treated with vehicle (old_veh). The right panel shows the *Usp21* l locus comparing exon usage in 3 (young_veh) and 18-month old mice treated with SAHA (old_SAHA). Note that the significant increase in exon usage seen in aged mice is normalized after SAHA treatment. * $p < 0.05$ GLM, n = 8 (YV), 6 (OV), 6 (OS). The *Usp21* locus is shown as it is regulated by aging (left) and after SAHA treatment (right). Arrow indicates the transcript annotated in ENSEMBL as nonsense-mediated decay.

Figure S8. The *Mapt* locus as an example of an exon inclusion that may be directly linked to pathology. The upper panel shows the *Mapt* locus comparing exon usage in 3 (young_veh) and 18-month old mice treated with vehicle (old_veh) . The middel panel shows the *Mapt* l locus comparing exon usage in 3 (young_veh) and 18-month old mice treated with SAHA (old_SAHA). Note that the significant increase in exon usage seen in aged mice is normalized after SAHA treatment. * $p < 0.05$ GLM, n = 8 (YV), 6 (OV), 6 (OS). The lower panel displays the structural features found in the different exons of the *Mapt gene* . Note that the significantly altered exons contain one of the four microtubule repeat domain that is essential for Tau binding to tubulin.

Figure S9. SAHA does not reinstate aberrant miRNA expression in age. A. Heatmap of aging-associated miRNA changes across all treatment conditions. Note that the physiological profile is not reinstated after SAHA treatment. **B.** Percentage of genes that are potentially targeted (based on predictions) by aging-upregulated/downregulated miRNAs within the aging-downregulated/upregulated mRNA population, respectively. **C.** Venn diagram (left) illustrating the effect of SAHA on miRNA expression (see also Table S6) and bar graphs depicting individual fold changes for SAHA-specific miRNAs (right).

Figure S10. STAT1 hyperactivation is partially reversed by SAHA. A. TFBS analysis (see methods for details) of aged animals with and without SAHA. **B.** Representative image of the

western blot signal for pSTAT1(S727). Bottom: quantification. * p <0.05, Student's t-test, n = 4 (YV), 5 (OV), 5 (OS); n.s., non-significant.

Please note there we measured phosphorylation of STAT1 since this is a reliable way to assess STAT1 activity. While STAT1/STAT3 acetylation has been demonstrated (Zhuang 2013), we did not find any commercial antibodies to probe this posttranslational mark in STAT1. We tested several antibodies for STAT3 acetylation but could not detect a reliable signal by western blotting.

Figure S11. Analysis of the aging- and SAHA-associated gene expression profile in liver. A. Number of significant up- and downregulated genes for aged and aged SAHA-treated animals. **B.** Overlaps of the aging signature in brain and liver for up- and downregulated genes. **C.** Overlaps and main functional terms associated with aging and SAHA in liver. **D-E.** An expanded view of the functionally enriched categories within aging-upregulated (D) or downregulated (E) genes in liver. **F-G.** Top GO terms associated with genes specifically up- or down-regulated in the direct OV vs. OS comparison. Note the predominance of metabolic terms. **H.** Number of differentially splice sites (exons and genes) in the indicated conditions. **I.** Percentage of expressed transcripts (defined as having >5 reads) in brain and liver in the indicated conditions.

Figure S12. Amyloid causes a transcriptional response that is concordant and augmented with respect to aging. A. Heatmap of genes induced by amyloid that are no longer significant after SAHA treatment. Each column represents a gene and each row a sample. **B.** Overlap of the core aging and amyloid signatures. Some of the top hits in both conditions are indicated. **C.** Fold changes in aging and amyloid for individual genes in the core of both responses. **D.** TFBS prediction on amyloid-upregulated genes and their significance.

Supplemental References

Anders, S., A. Reyes and W. Huber (2012). "Detecting differential usage of exons from RNA-seq data." Genome Res **22**(10): 2008-2017.

Djebali, S., C. A. Davis, A. Merkel, A. Dobin, T. Lassmann, A. Mortazavi, A. Tanzer, J. Lagarde and W. S. F. Lin, Xue C, Marinov GK, Khatun J, Williams BA, Zaleski C, Rozowsky J, Röder M, Kokocinski F, Abdelhamid RF, Alioto T, Antoshechkin I, Baer MT, Bar NS, Batut P, Bell K, Bell I, Chakrabortty S, Chen X, Chrast J, Curado J, Derrien T, Drenkow J, Dumais E, Dumais J, Duttagupta R, Falconnet E, Fastuca M, Fejes-Toth K, Ferreira P, Foissac S, Fullwood MJ, Gao H, Gonzalez D, Gordon A, Gunawardena H, Howald C, Jha S, Johnson R, Kapranov P, King B, Kingswood C, Luo OJ, Park E, Persaud K, Preall JB, Ribeca P, Risk B, Robyr D, Sammeth M, Schaffer L, See LH, Shahab A, Skancke J, Suzuki AM, Takahashi H, Tilgner H, Trout D, Walters N, Wang H, Wrobel J, Yu Y, Ruan X, Hayashizaki Y, Harrow J, Gerstein M, Hubbard T, Reymond A, Antonarakis SE, Hannon G, Giddings MC, Ruan Y, Wold B, Carninci P, Guigó R, Gingeras TR. (2012). "Landscape of transcription in human cells." Nature **489**(7414): 101-108.

Hagihara, H., K. Toyama, N. Yamasaki and T. Miyakawa (2009). "Dissection of hippocampal dentate gyrus from adult mouse." J Vis Exp(33).

Hu Zhi-Liang, B. J., Reecy JM (2008). "CateGOrizer: A Web-Based Program to Batch Analyze Gene Ontology Classification Categories." Online Journal of Bioinformatics **9**(2): 108-112.

Huang, D. W., B. T. Sherman and R. A. Lempicki (2009). "Systematic and integrative analysis of large gene lists using DAVID Bioinformatics Resources." Nature Protoc **4**(1): 44-57.

Kerimoglu, C., R. C. Agis-Balboa, A. Kranz, R. Stilling, S. Bahari-Javan, E. Benito-Garagorri, R. Halder, S. Burkhardt, A. F. Stewart and A. Fischer (2013). "Histone-methyltransferase MLL2 (KMT2B) is required for memory formation in mice." J Neurosci **33**(8): 3452-3464.

Kuroda, H., R. H. Kutner, N. G. Bazan and J. Reiser (2009). "Simplified lentivirus vector production in protein-free media using polyethylenimine-mediated transfection." J Virol Methods **157**(2): 113-121.

Lawrence, M., W. Huber, H. Pages, P. Aboyoun, M. Carlson, R. Gentleman, M. T. Morgan and V. J. Carey (2013). "Software for computing and annotating genomic ranges." PLoS Comput Biol **9**(8): e1003118.

Li, H., B. Handsaker, A. Wysoker, T. Fennell, J. Ruan, N. Homer, G. Marth, G. Abecasis, R. Durbin and S. Genome Project Data Processing (2009). "The Sequence Alignment/Map format and SAMtools." Bioinformatics **25**(16): 2078-2079.

M. I. Love, W. H., S. Anders (2014). "Moderated estimation of fold change and dispersion for RNA-Seq data with DESeq2." bioRxiv.

Ramachandran, B. and J. U. Frey (2009). "Interfering with the actin network and its effect on long-term potentiation and synaptic tagging in hippocampal CA1 neurons in slices in vitro." J Neurosci **29**(39): 12167-12173.

Zambelli, F., G. Pesole and G. Pavesi (2009). "Pscan: finding over-represented transcription factor binding site motifs in sequences from co-regulated or co-expressed genes." Nucleic Acids Res **37**(Web Server issue): W247-252.

Zhang, B., S. Kirov and J. Snoddy (2005). "WebGestalt: an integrated system for exploring gene sets in various biological contexts." Nucleic Acids Res **33**(Web Server issue): W741-748.

Zhuang, S. (2013). "Regulation of STAT signaling by acetylation." Cell Signal **25**(9): 1924-1931.

Fig S1

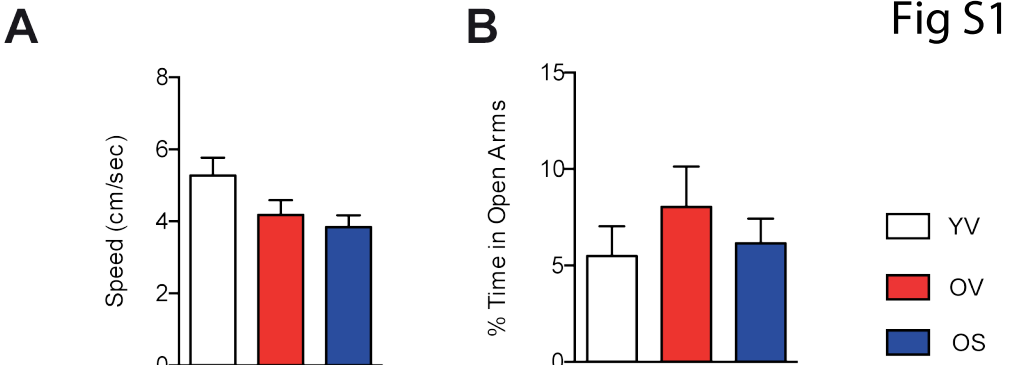

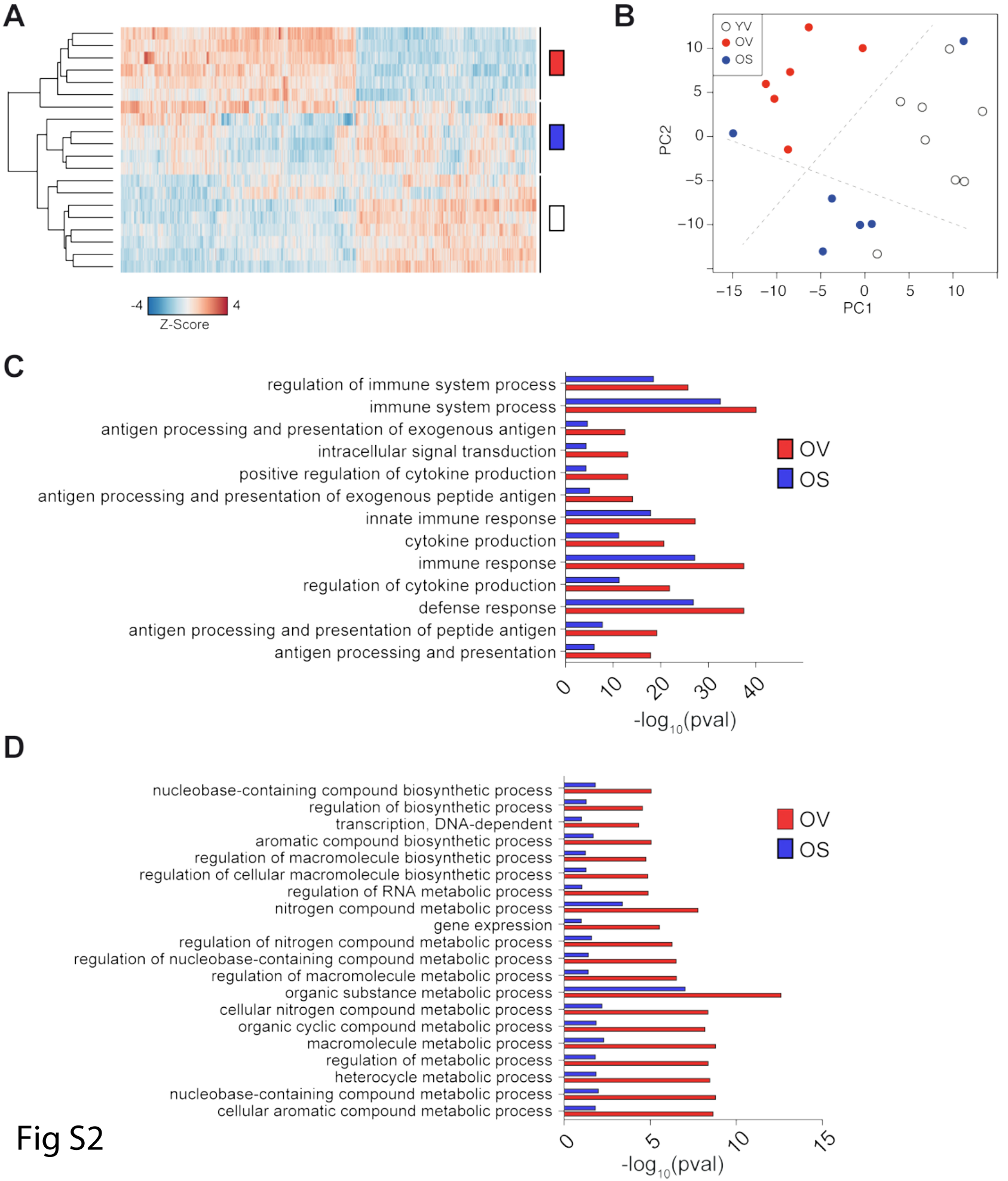
A
-4
4
Z-Score
B
YV
OV
OS
PC2
PC1
C
regulation of immune system process
immune system process
antigen processing and presentation of exogenous antigen
intracellular signal transduction
positive regulation of cytokine production
antigen processing and presentation of exogenous peptide antigen
innate immune response
cytokine production
immune response
regulation of cytokine production
defense response
antigen processing and presentation of peptide antigen
antigen processing and presentation
OV
OS
-log10(pval)
D
nucleobase-containing compound biosynthetic process
regulation of biosynthetic process
transcription, DNA-dependent
aromatic compound biosynthetic process
regulation of macromolecule biosynthetic process
regulation of cellular macromolecule biosynthetic process
regulation of RNA metabolic process
nitrogen compound metabolic process
gene expression
regulation of nitrogen compound metabolic process
regulation of nucleobase-containing compound metabolic process
regulation of macromolecule metabolic process
organic substance metabolic process
cellular nitrogen compound metabolic process
organic cyclic compound metabolic process
macromolecule metabolic process
regulation of metabolic process
heterocycle metabolic process
nucleobase-containing compound metabolic process
cellular aromatic compound metabolic process
OV
OS
-log10(pval)

Fig S2

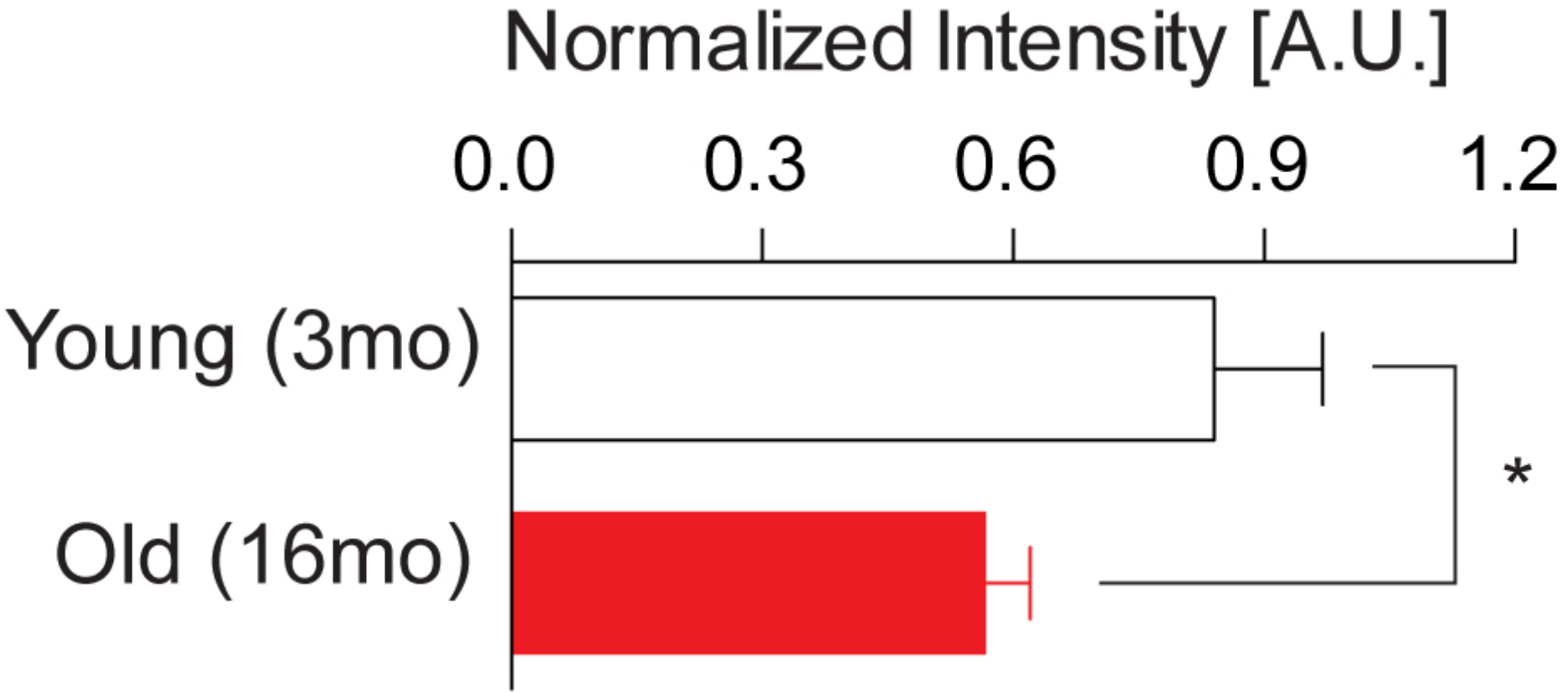

Fig S3

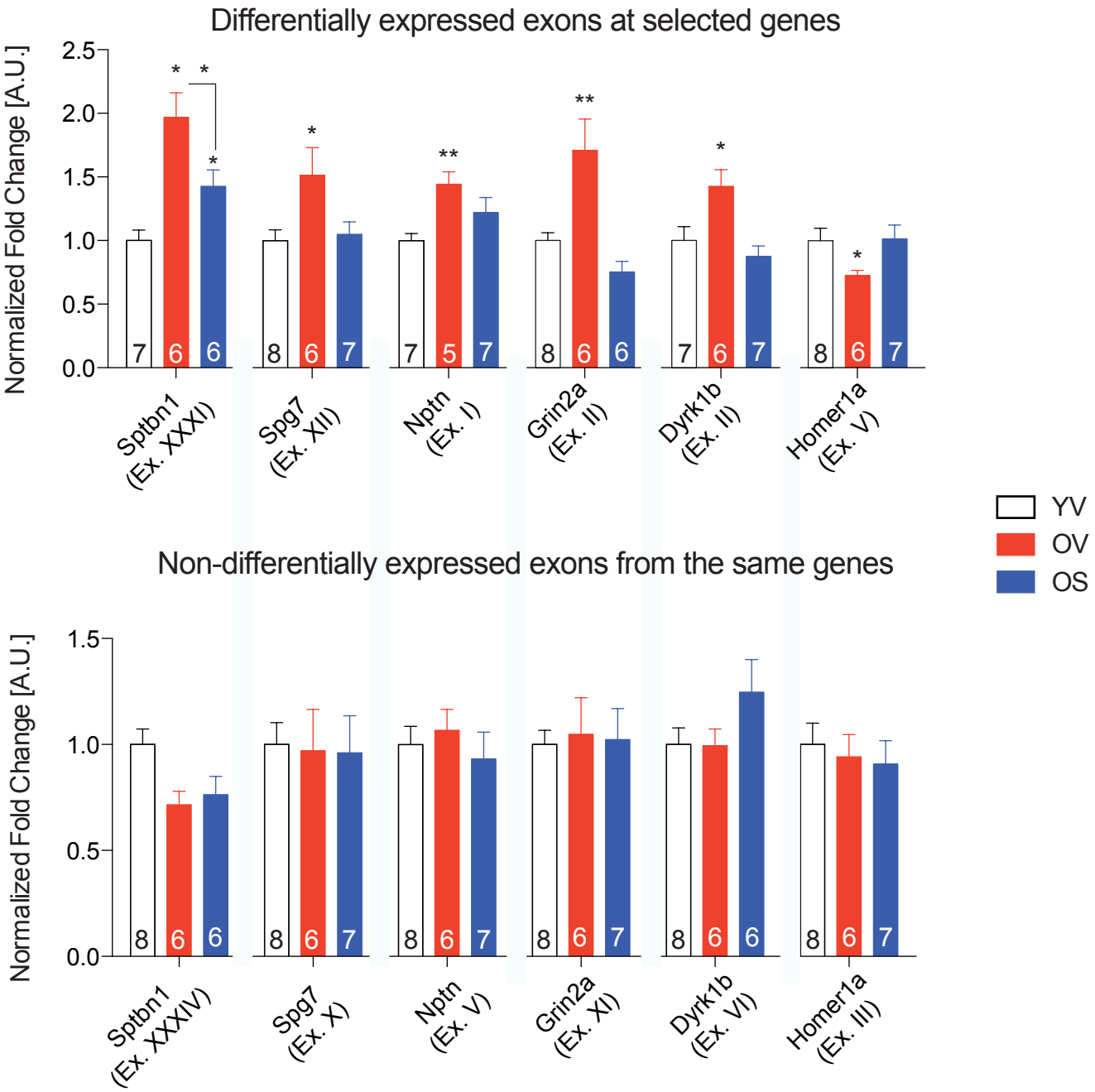
Differentially expressed exons at selected genes
Normalized Fold Change [A.U.]
2.5
2.0
1.5
1.0
0.5
0.0
* * *
*
**
*
*
7 6 6
8 6 7
7 5 7
8 6 6
7 6 7
8 6 7
Sptbn1 (Ex. XXXI)
Spg7 (Ex. XII)
Nptn (Ex. I)
Grin2a (Ex. II)
Dyrk1b (Ex. II)
Homer1a (Ex. V)
YV
OV
OS
Non-differentially expressed exons from the same genes
Normalized Fold Change [A.U.]
1.5
1.0
0.5
0.0
8 6 6
8 6 7
8 6 7
8 6 7
8 6 6
8 6 7
Sptbn1 (Ex. XXXIV)
Spg7 (Ex. X)
Nptn (Ex. V)
Grin2a (Ex. XI)
Dyrk1b (Ex. VI)
Homer1a (Ex. III)

Fig S5

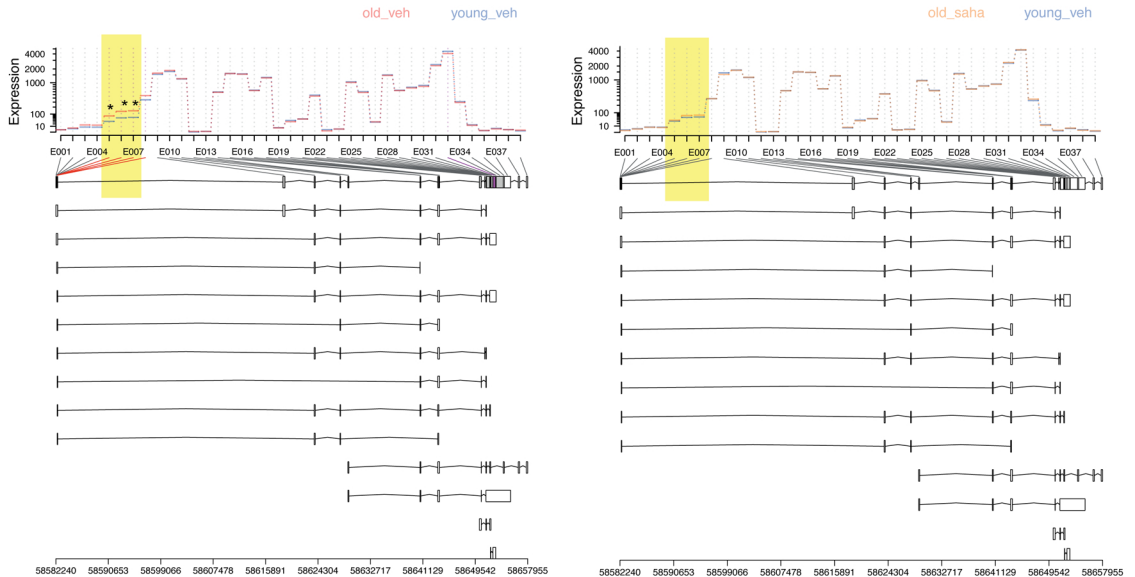
ENSMUSG00000032336 - Neuroplastin
old_veh
young_veh
old_saha
young_veh
Expression
4000
2000
1000
100
10
*
* *
E001 E004 E007 E010 E013 E016 E019 E022 E025 E028 E031 E034 E037
58582240 58590653 58599066 58607478 58615891 58624304 58632717 58641129 58649542 58657955
8413bp

Fig S6

Sptbn1

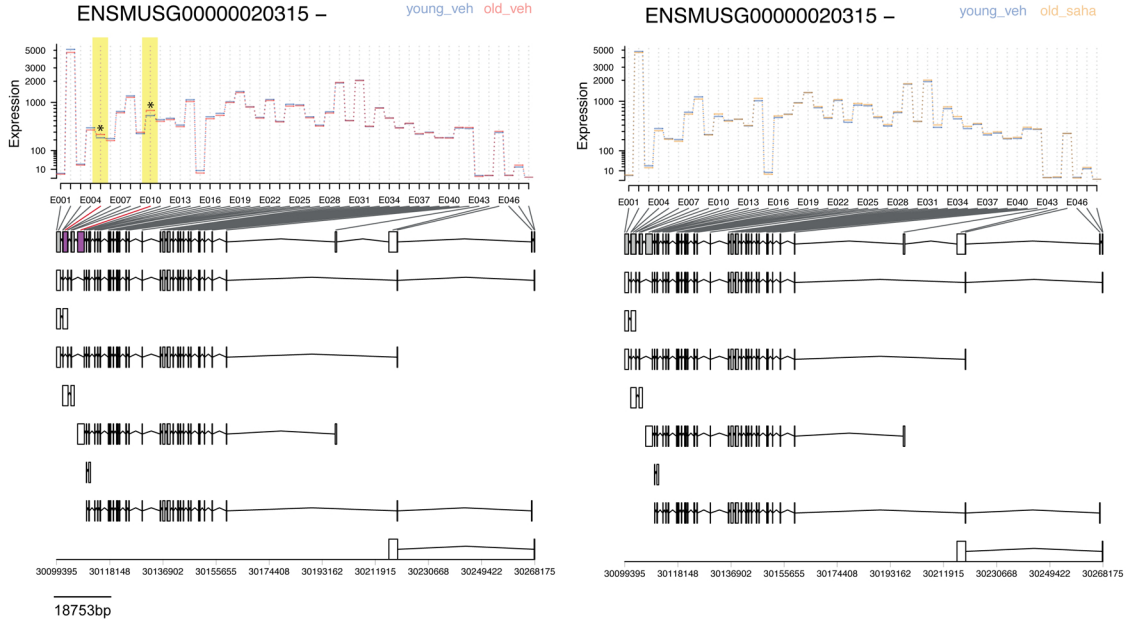

Fig S7

Usp21

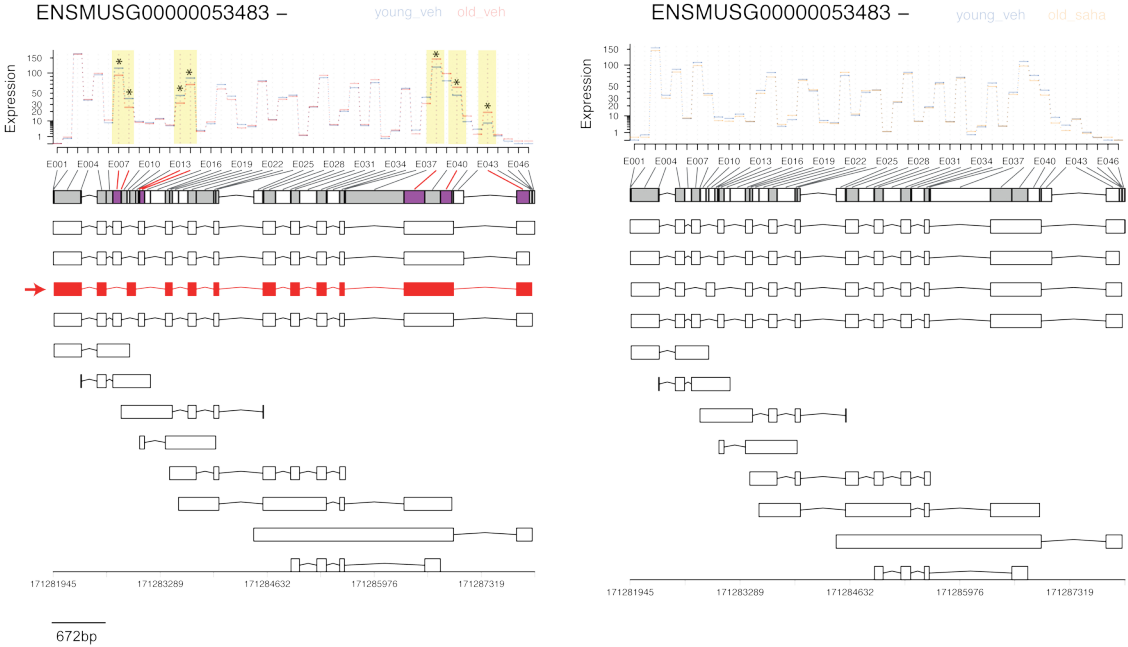
ENSMUSG00000053483 –
young_veh
old_veh
Expression
150
100
50
30
20
10
1
E001 E004 E007 E010 E013 E016 E019 E022 E025 E028 E031 E034 E037 E040 E043 E046
171281945
171283289
171284632
171285976
171287319
672bp
ENSMUSG00000053483 –
young_veh
old_saha
Expression
150
100
50
30
20
10
1
E001 E004 E007 E010 E013 E016 E019 E022 E025 E028 E031 E034 E037 E040 E043 E046
171281945
171283289
171284632
171285976
171287319

Fig S8

Mapt

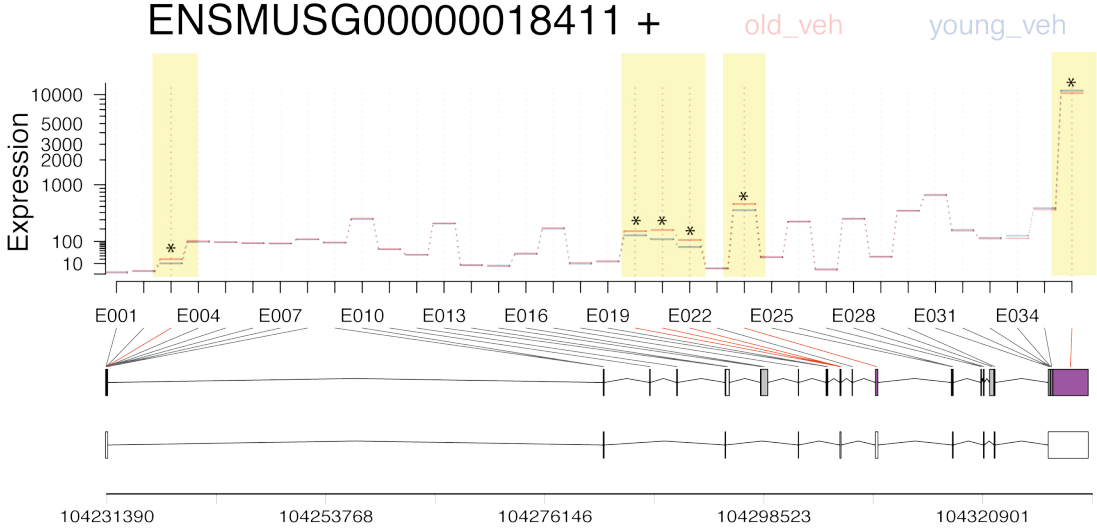
ENSMUSG00000018411 +
old_veh
young_veh
Expression
10000
5000
3000
2000
1000
100
10
E001
E004
E007
E010
E013
E016
E019
E022
E025
E028
E031
E034
104231390
104253768
104276146
104298523
104320901
11189bp

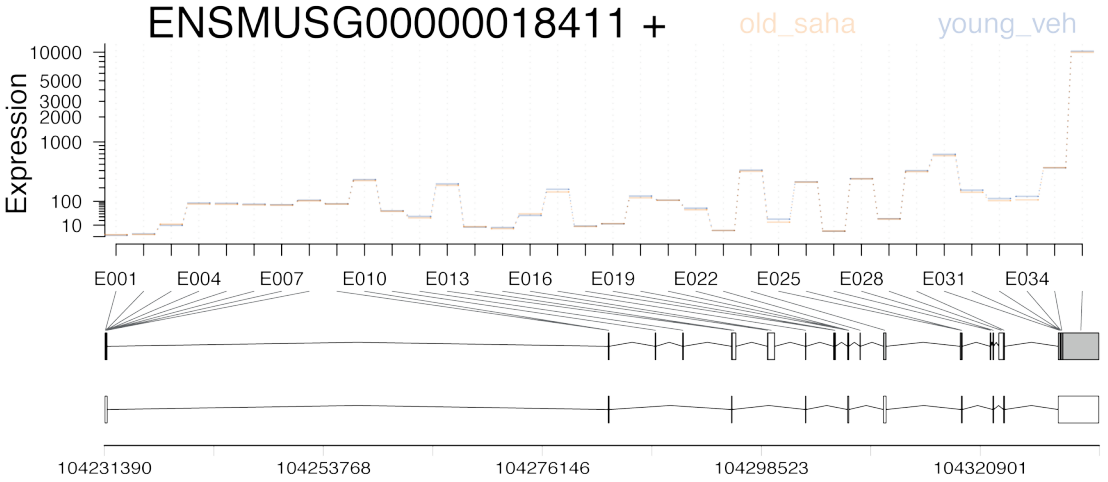
ENSMUSG00000018411 +
old_saha
young_veh
Expression
10000
5000
3000
2000
1000
100
10
E001
E004
E007
E010
E013
E016
E019
E022
E025
E028
E031
E034
104231390
104253768
104276146
104298523
104320901

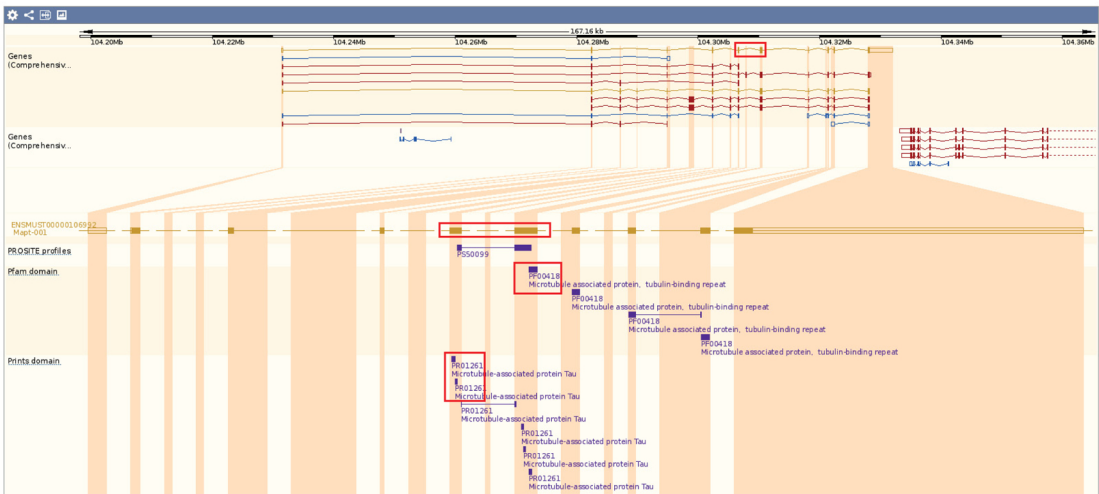
Genes (Comprehensiv...
Genes (Comprehensiv...
PROSITE profiles
Pfam domain
Prints domain
PS50099
PF00418
Microtubule associated protein, tubulin-binding repeat
PR01261
Microtubule-associated protein Tau
PR01262
Microtubule-associated protein Tau

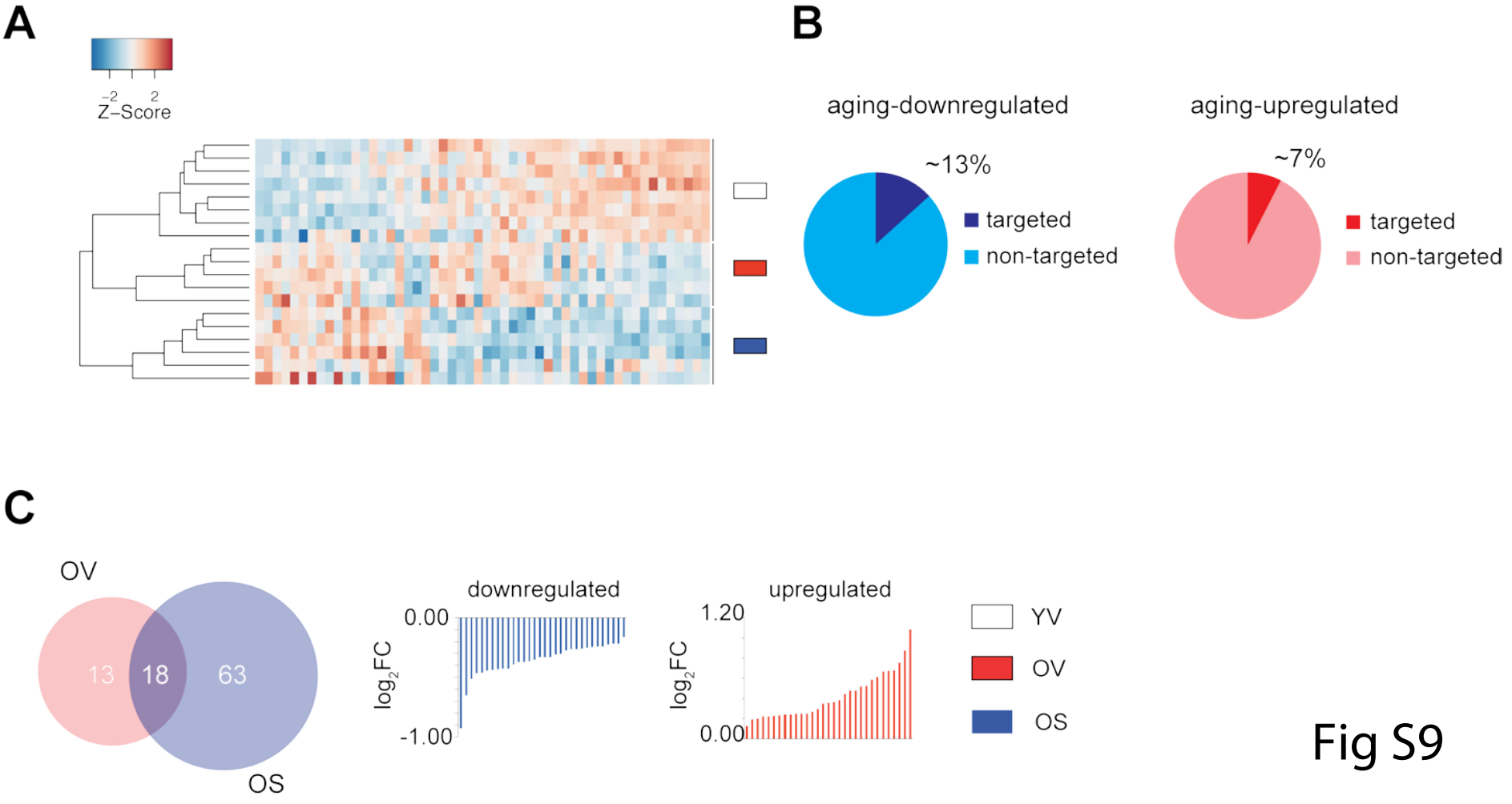
A
−2
2
Z−Score
B
aging-downregulated
~13%
targeted
non-targeted
aging-upregulated
~7%
targeted
non-targeted
C
OV
13
18
63
OS
downregulated
0.00
-1.00
log2FC
upregulated
1.20
0.00
log2FC
YV
OV
OS

Fig S9

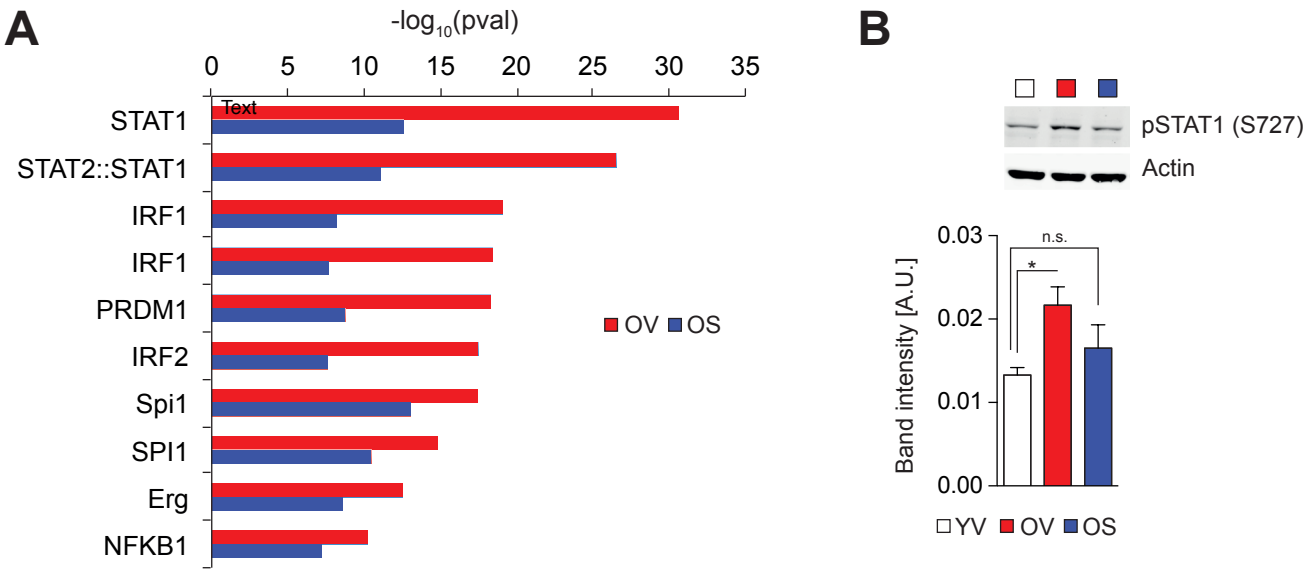
A
-log10(pval)
0
5
10
15
20
25
30
35
Text
STAT1
STAT2::STAT1
IRF1
IRF1
PRDM1
IRF2
Spi1
SPI1
Erg
NFKB1
OV
OS
B
pSTAT1 (S727)
Actin
Band intensity [A.U.]
0.03
0.02
0.01
0.00
n.s.
*
YV
OV
OS

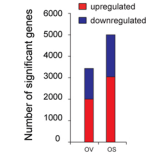
A
upregulated
downregulated
Number of significant genes
6000
5000
4000
3000
2000
1000
0
ov
os

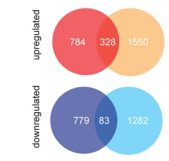
B
brain
liver
upregulated
downregulated
784
328
1550
779
83
1282

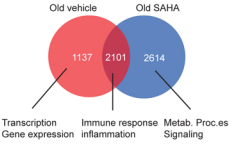
C
Old vehicle
Old SAHA
1137
2101
2614
Transcription
Gene expression
Immune response
inflammation
Metab. Proc.es
Signaling

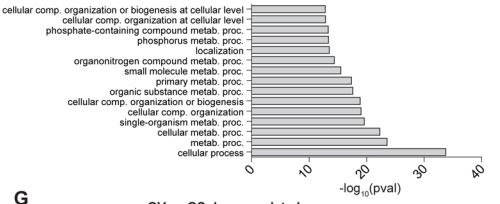
F
OV vs OS upregulated
cellular comp. organization or biogenesis at cellular level
cellular comp. organization at cellular level
phosphate-containing compound metab. proc.
phosphorus metab. proc.
localization
organonitrogen compound metab. proc.
small molecule metab. proc.
primary metab. proc.
organic substance metab. proc.
cellular comp. organization or biogenesis
cellular comp. organization
single-organism metab. proc.
cellular metab. proc.
metab. proc.
cellular process
0
10
20
30
40
-log10(pval)

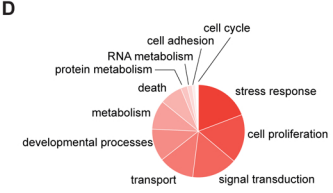
D
cell cycle
cell adhesion
RNA metabolism
protein metabolism
death
metabolism
developmental processes
transport
signal transduction
stress response
cell proliferation

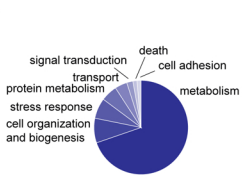
E
signal transduction
death
cell adhesion
transport
protein metabolism
stress response
cell organization
and biogenesis
metabolism

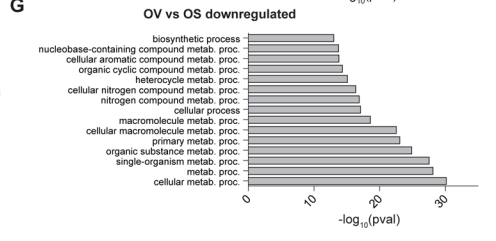
G
OV vs OS downregulated
biosynthetic process
nucleobase-containing compound metab. proc.
cellular aromatic compound metab. proc.
organic cyclic compound metab. proc.
heterocycle metab. proc.
cellular nitrogen compound metab. proc.
nitrogen compound metab. proc.
cellular process
macromolecule metab. proc.
cellular macromolecule metab. proc.
primary metab. proc.
organic substance metab. proc.
single-organism metab. proc.
metab. proc.
cellular metab. proc.
0
10
20
30
-log10(pval)

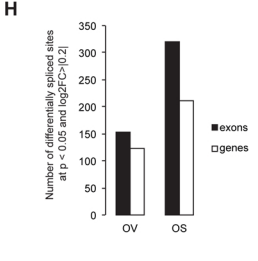
H
Number of differentially spliced sites
at p < 0.05 and log2FC>|0.2|
350
300
250
200
150
100
50
0
exons
genes
OV
OS

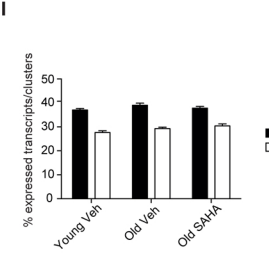
I
% expressed transcripts/clusters
50
40
30
20
10
0
Brain
Liver
Young Veh
Old Veh
Old SAHA

Fig S11

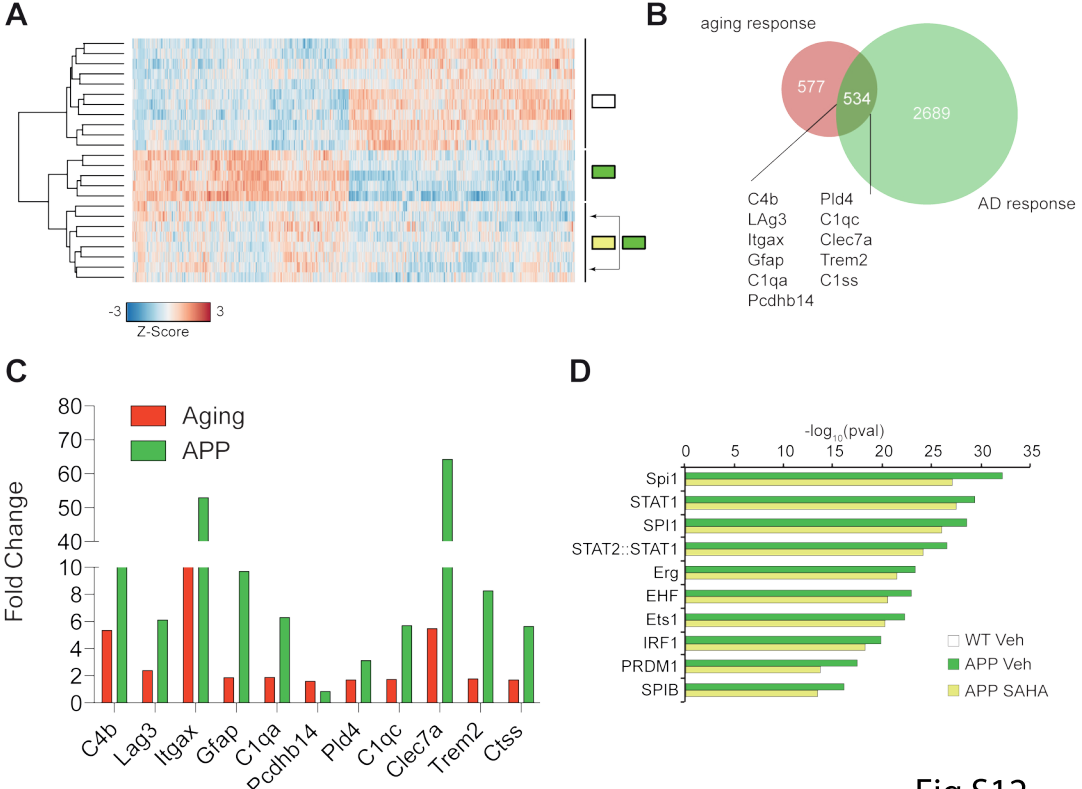
A
-3
3
Z-Score
B
aging response
577
534
2689
AD response
C4b
LAg3
Itgax
Gfap
C1qa
Pcdhb14
Pld4
C1qc
Clec7a
Trem2
C1ss
C
Aging
APP
Fold Change
80
70
60
50
40
10
8
6
4
2
0
C4b
Lag3
Itgax
Gfap
C1qa
Pcdhb14
Pld4
C1qc
Clec7a
Trem2
Ctss
D
-log10(pval)
0
5
10
15
20
25
30
35
Spi1
STAT1
SPI1
STAT2::STAT1
Erg
EHF
Ets1
IRF1
PRDM1
SPIB
WT Veh
APP Veh
APP SAHA

Fig S12